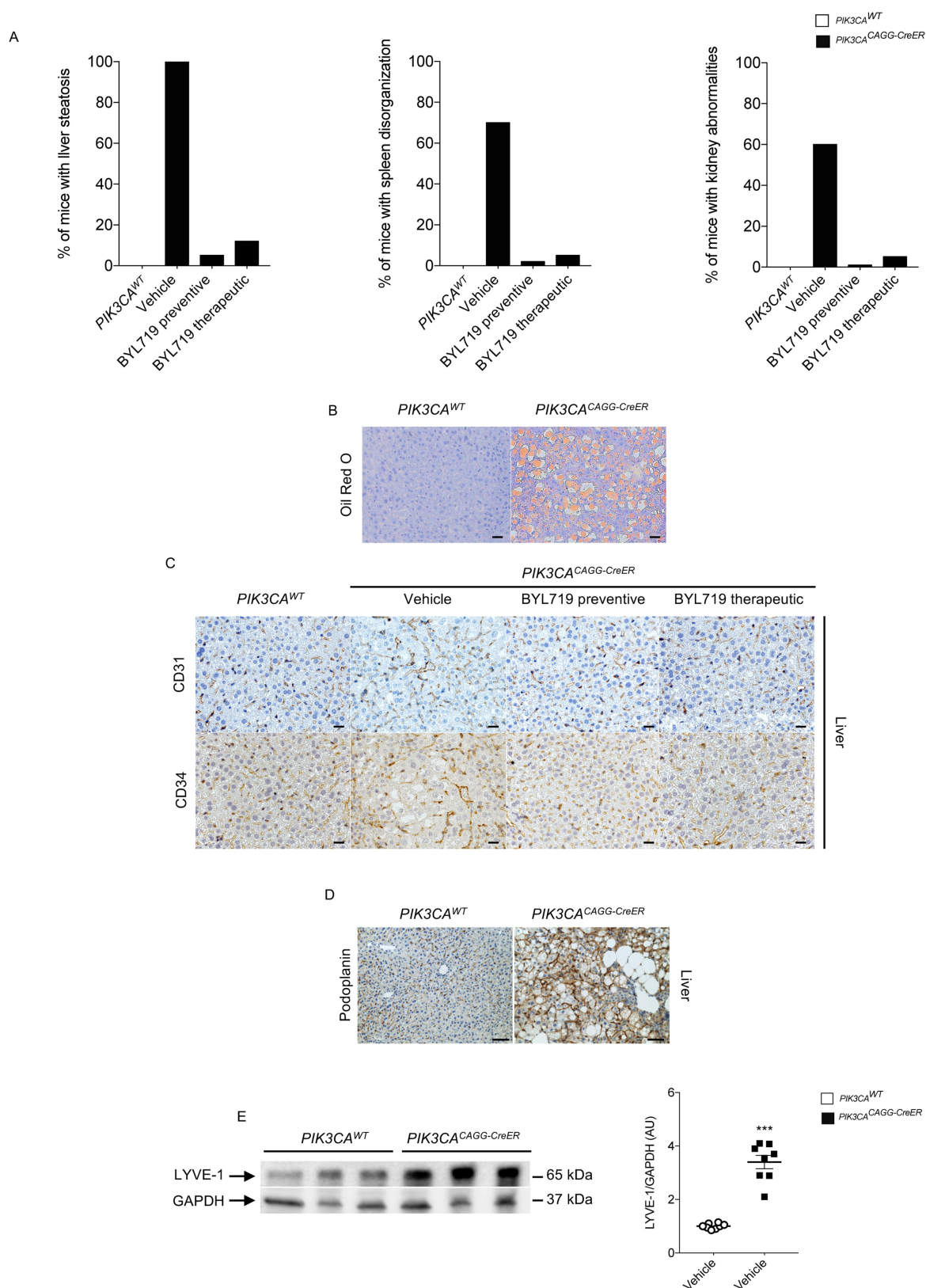


Extended Data Fig. 1 | See next page for caption.

Extended Data Fig. 1 | p110* construction and mouse model characterization. **a**, Left, Representation of p110 and iSH2 domain of the p85 subunit (striped bar). The iSH2 domain is important to stabilize the p110 α protein. The p110* protein is a constitutively active chimera that contains the iSH2 domain of p85 fused to the N terminus of p110 via a flexible glycine linker¹⁴ (right). **b**, To generate tissue-specific p110*-transgenic mice, a cloned loxP-flanked neoR-stop cassette was inserted into a modified version of pROSA26-1 followed by the cDNA encoding p110* and then a frt-flanked IRES-EGFP cassette and a bovine polyadenylation sequence (*R26StopFLP110**)¹³. **c**, **d**, EGFP expression from flow cytometry experiments in the spleen of *PIK3CA*^{WT}

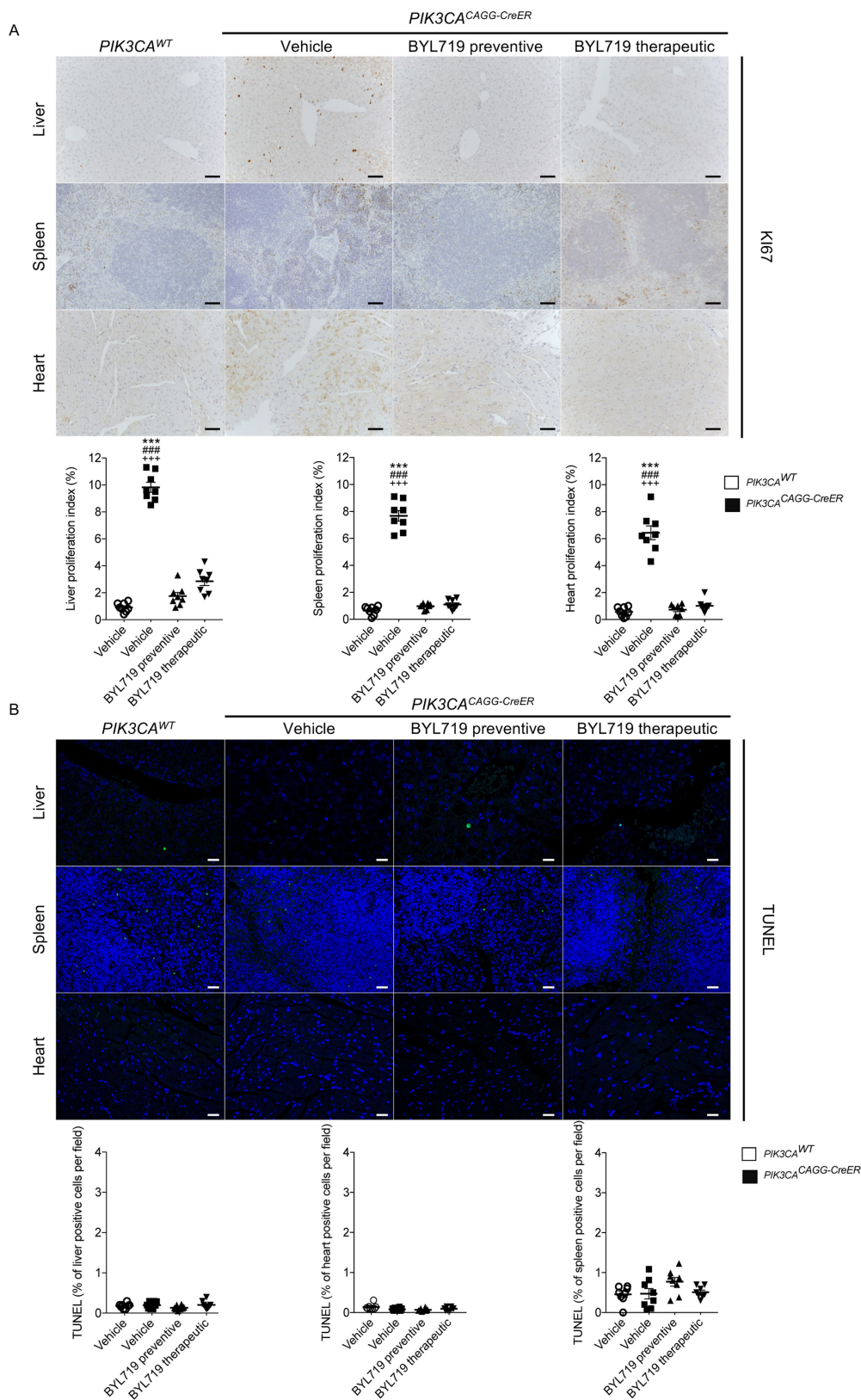
mice ($n = 12$) and *PIK3CA*^{CAGG-CreER} mice injected with either a single 40 mg kg⁻¹ dose (**c**; $n = 6$ mice) or a single 4 mg kg⁻¹ dose (**d**; $n = 6$ mice) of tamoxifen. Each curve is a different mouse. **e**, MRI examination of the PROS mouse model and efficacy of BYL719 treatment. Top, arrows show muscle hypertrophy in *PIK3CA*^{CAGG-CreER} mice before BYL719 treatment. This phenotype was reversed by BYL719 administration. Middle, arrows show scoliosis in *PIK3CA*^{CAGG-CreER} mice before BYL719 treatment, which was rescued by BYL719 administration. Bottom, arrows show arterial dilation in *PIK3CA*^{CAGG-CreER} mice before BYL719 treatment, which was reversed by BYL719 administration ($n = 6$ mice per group).



Extended Data Fig. 2 | Quantification and vessel malformation.

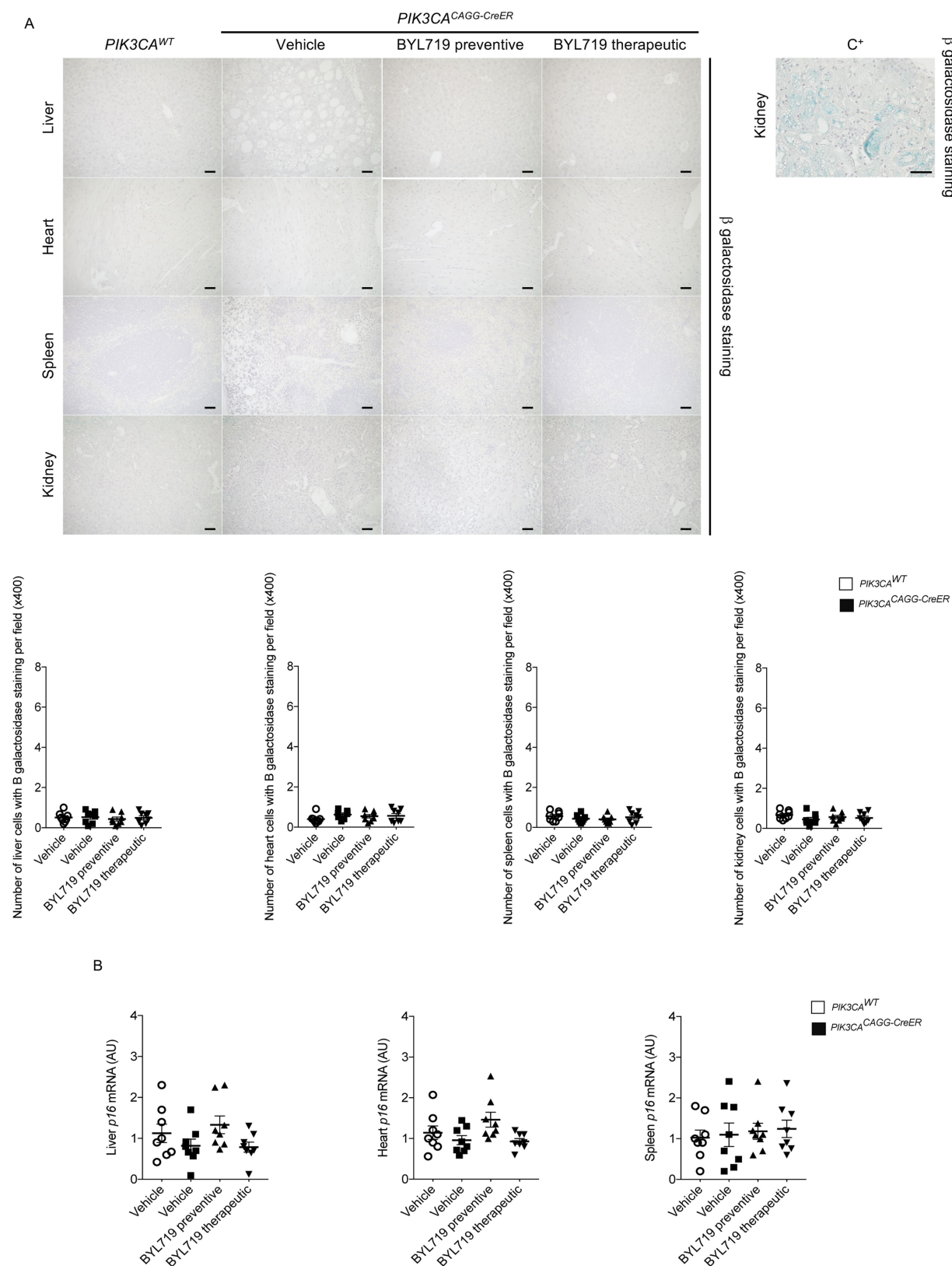
a, Percentage of *PIK3CA*^{WT} and *PIK3CA*^{CAGG-CreER} mice with or without BYL719 treatment presenting organ abnormalities. **b**, Oil Red O staining of the livers of *PIK3CA*^{WT} and *PIK3CA*^{CAGG-CreER} mice demonstrating steatosis ($n = 8$ mice per group). Scale bars, 10 μ m. **c**, CD31 (top) and CD34 (bottom) immunostaining in the liver of *PIK3CA*^{WT} and *PIK3CA*^{CAGG-CreER} mice with or without BYL719 ($n = 8$ mice per group). *PIK3CA*^{CAGG-CreER} mice treated with vehicle showed vessel dilation that was prevented or reversed by BYL719. Scale bars, 10 μ m. **d**, Representative

picture of lymphatic malformation as assessed by podoplanin immunostaining in the liver of *PIK3CA*^{WT} and *PIK3CA*^{CAGG-CreER} mice ($n = 8$ mice per group). Scale bars, 10 μ m. **e**, Representative western blot of LYVE-1 in the liver of *PIK3CA*^{WT} and *PIK3CA*^{CAGG-CreER} mice demonstrating lymphatic increased in the *PIK3CA*^{CAGG-CreER} mice ($n = 8$ mice per group). All data are shown as the means \pm s.e.m. Mann-Whitney test (two-tailed, $P = 0.001$). *PIK3CA*^{CAGG-CreER} versus *PIK3CA*^{WT} mice, *** $P < 0.001$.



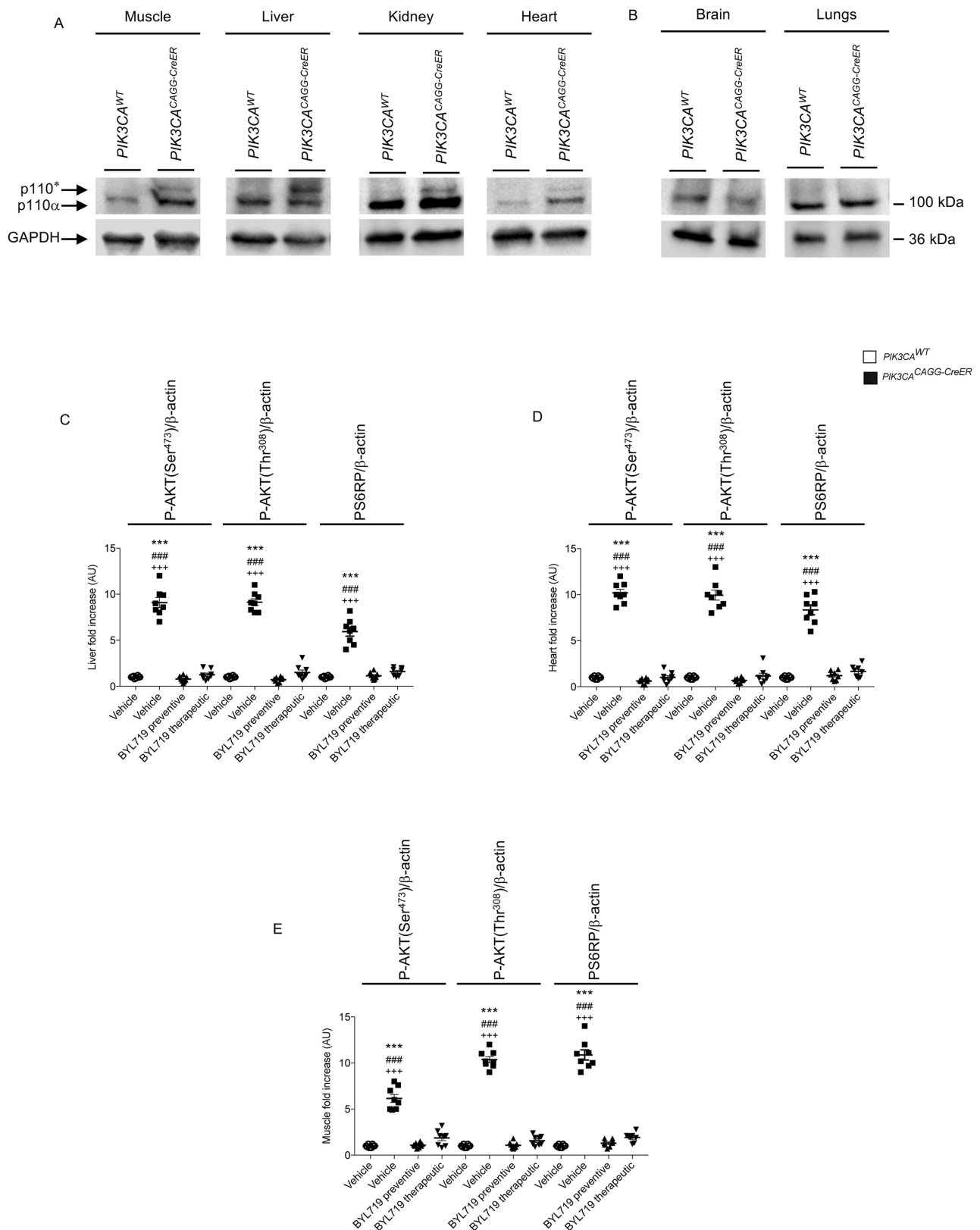
Extended Data Fig. 3 | BYL719 affects proliferation. **a**, Ki67 immunostaining and quantification in liver, spleen and heart of *PIK3CA*^{WT} and *PIK3CA*^{CAGG-CreER} mice with or without BYL719 treatment (*n* = 8 mice per group, 10 randomly selected fields per mice, ×400). **b**, TUNEL assay. The graphs show the quantification of TUNEL-positive cells per field (*n* = 8 mice per group, 10 randomly selected fields per mice, ×400).

Scale bars, 10 μm . All data are shown as mean \pm s.e.m. ANOVA followed by Tukey–Kramer test (two-tailed). *PIK3CA*^{CAGG-CreER} versus *PIK3CA*^{WT} mice, *** $P < 0.001$. *PIK3CA*^{CAGG-CreER} mice treated with vehicle versus *PIK3CA*^{CAGG-CreER} mice treated with preventive BYL719, ### $P < 0.001$. *PIK3CA*^{CAGG-CreER} mice treated with vehicle versus *PIK3CA*^{CAGG-CreER} mice treated with therapeutic BYL719, +++ $P < 0.001$.



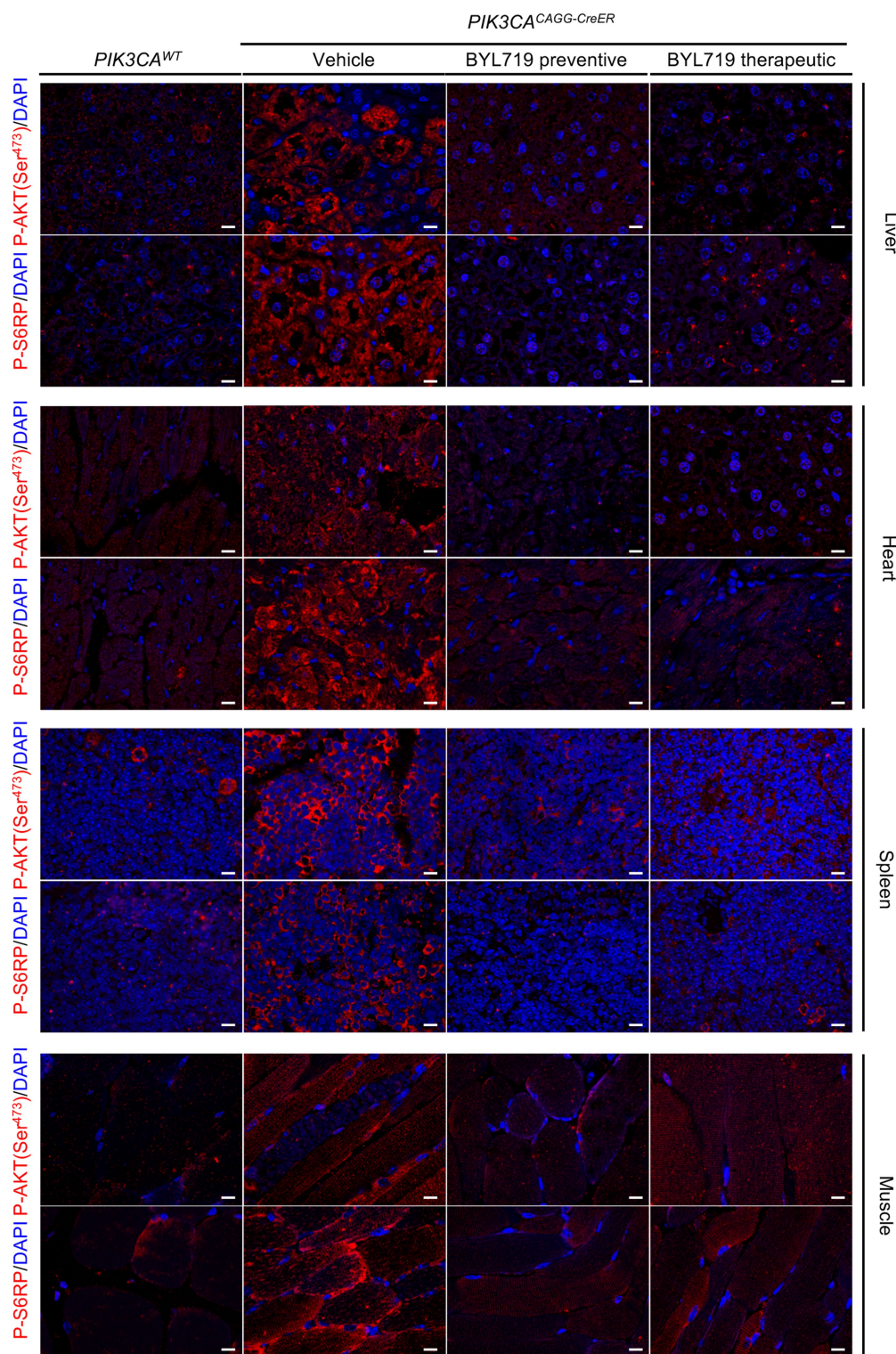
Extended Data Fig. 4 | Senescence and BYL719. **a**, β -galactosidase staining in the liver, spleen and kidney of *PIK3CA*^{WT} and *PIK3CA*^{CAGG-CreER} mice with or without BYL719 and quantification of β -galactosidase-positive cells per field ($n = 8$ mice per group, 10 randomly selected fields, $\times 400$). C⁺: positive control. Scale bars, 10 μ m.

b, *p16* mRNA expression in liver, heart and spleen of *PIK3CA*^{WT} and *PIK3CA*^{CAGG-CreER} mice treated with or without BYL719 ($n = 8$ mice per group). A.U., arbitrary unit. All data are shown as mean \pm s.e.m. ANOVA followed by Tukey-Kramer test (two-tailed).



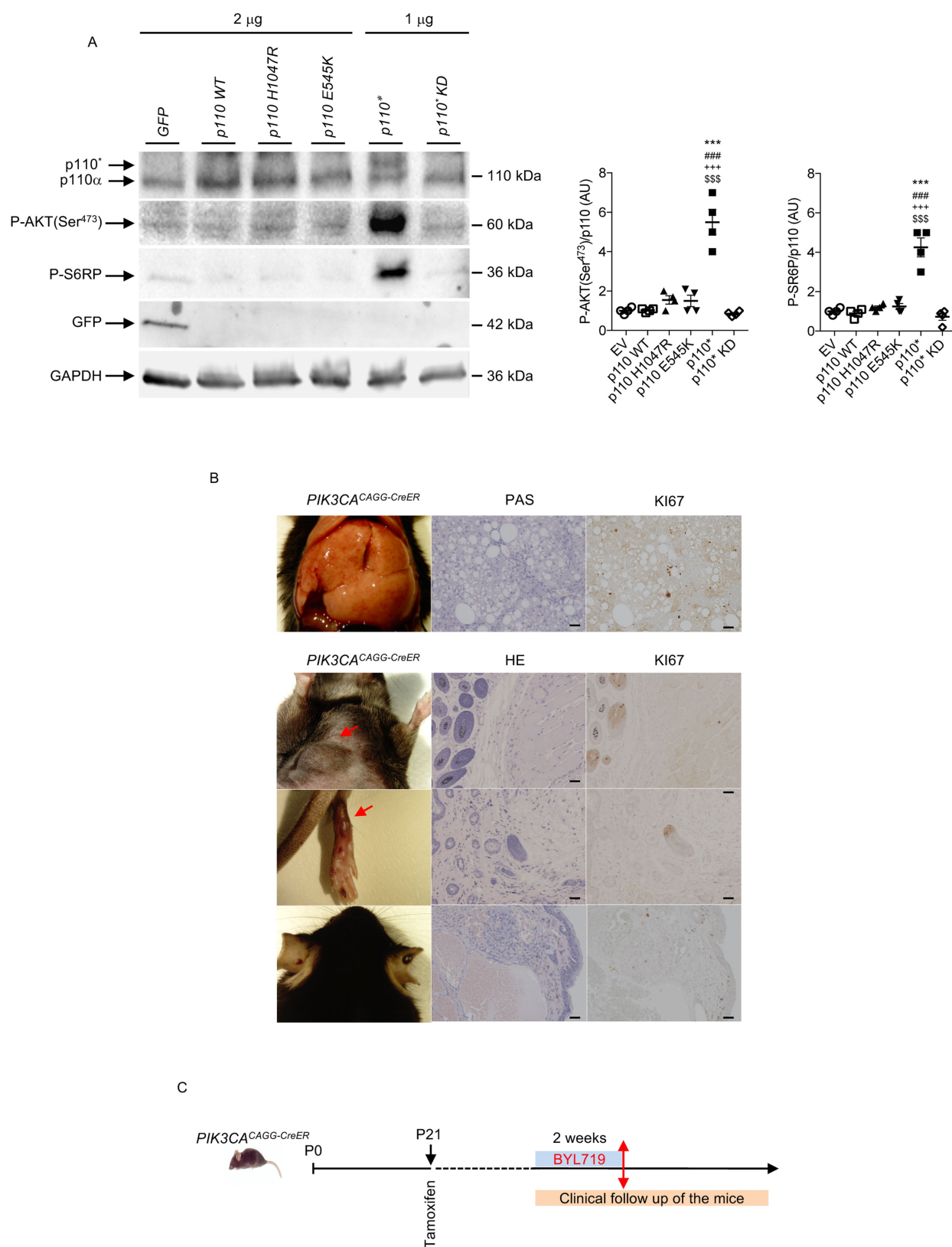
Extended Data Fig. 5 | p110* expression in affected tissues. a, Western blot showing the expression of p110* in *PIK3CA*^{CAGG-CreER} mice ($n = 8$ mice per group). **b**, p110* is not expressed in the brain or lungs ($n = 8$ mice per group). **c–e**, Western blot quantification of Fig. 1d, in the liver (**c**), heart (**d**) and muscle (**e**) of *PIK3CA*^{WT} and *PIK3CA*^{CAGG-CreER} mice treated with or without BYL719 ($n = 8$ mice per group). All data are shown as

mean \pm s.e.m. ANOVA followed by Tukey–Kramer test (two-tailed). *PIK3CA*^{CAGG-CreER} versus *PIK3CA*^{WT} mice, *** $P < 0.001$. *PIK3CA*^{CAGG-CreER} mice treated with vehicle versus *PIK3CA*^{CAGG-CreER} mice treated with preventive BYL719, ### $P < 0.001$. *PIK3CA*^{CAGG-CreER} mice treated with vehicle versus *PIK3CA*^{CAGG-CreER} mice treated with therapeutic BYL719, +++ $P < 0.001$.



Extended Data Fig. 6 | Ability of BYL719 to inhibit PIK3CA activation in different tissues. Immunofluorescence staining of P-AKT (Ser⁴⁷³) and P-S6RP in the liver (a), heart (b), spleen (c) and muscles (d) of *PIK3CA*^{WT}

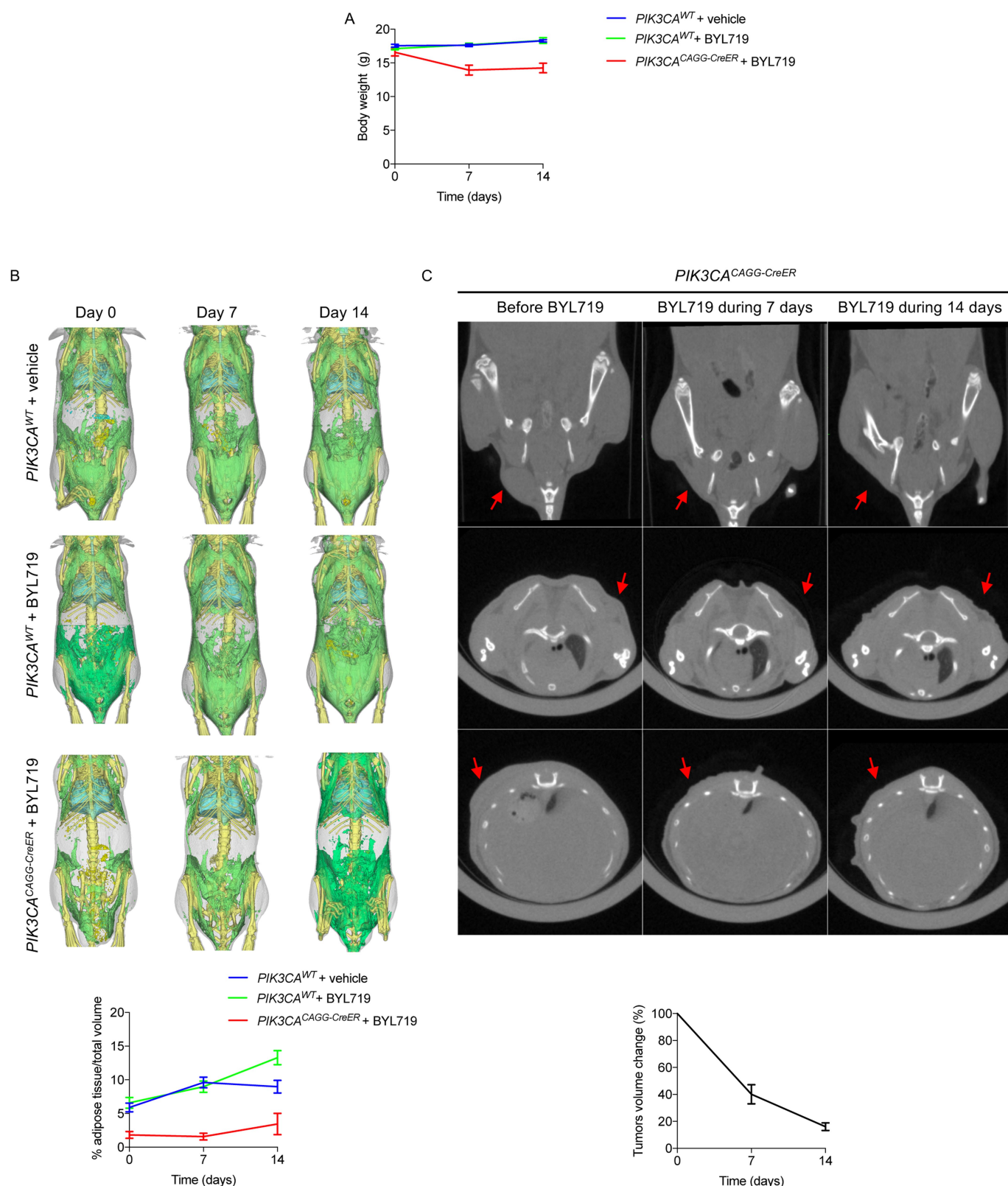
and *PIK3CA*^{CAGG-CreER} mice treated with or without BYL719 ($n = 8$ mice per group). Scale bars, 10 μ m.

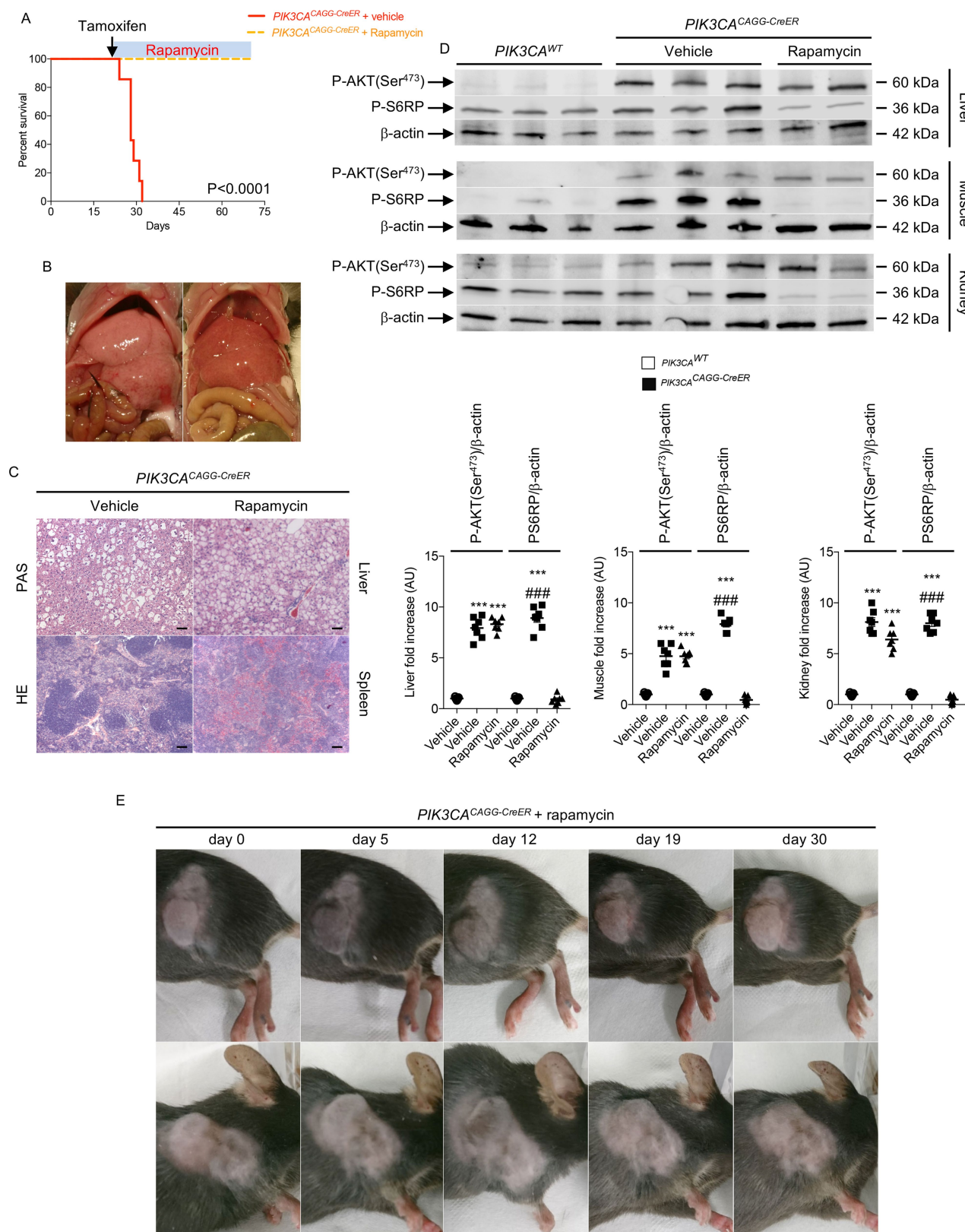


Extended Data Fig. 7 | See next page for caption.

Extended Data Fig. 7 | Recruitment of the AKT/mTORC pathway by the different forms of mutant p110. **a**, Western blot and quantification of p110, P-AKT (Ser⁴⁷³), P-S6RP and GFP in HeLa cells transfected with plasmids containing cDNA encoding p110*, p110* kinase-dead mutant (p110* KD) as a control, H1047R mutation or E545K mutation. Cells transfected with the p110* mutant showed a more powerful effect on the activation of the AKT/mTORC pathway than the others ($n = 4$ independent experiments). All data are shown as mean \pm s.e.m. ANOVA followed by Tukey–Kramer test (two-tailed). p110* versus H1047R mutation, *** $P < 0.001$. p110* versus E545K mutation, ### $P < 0.001$.

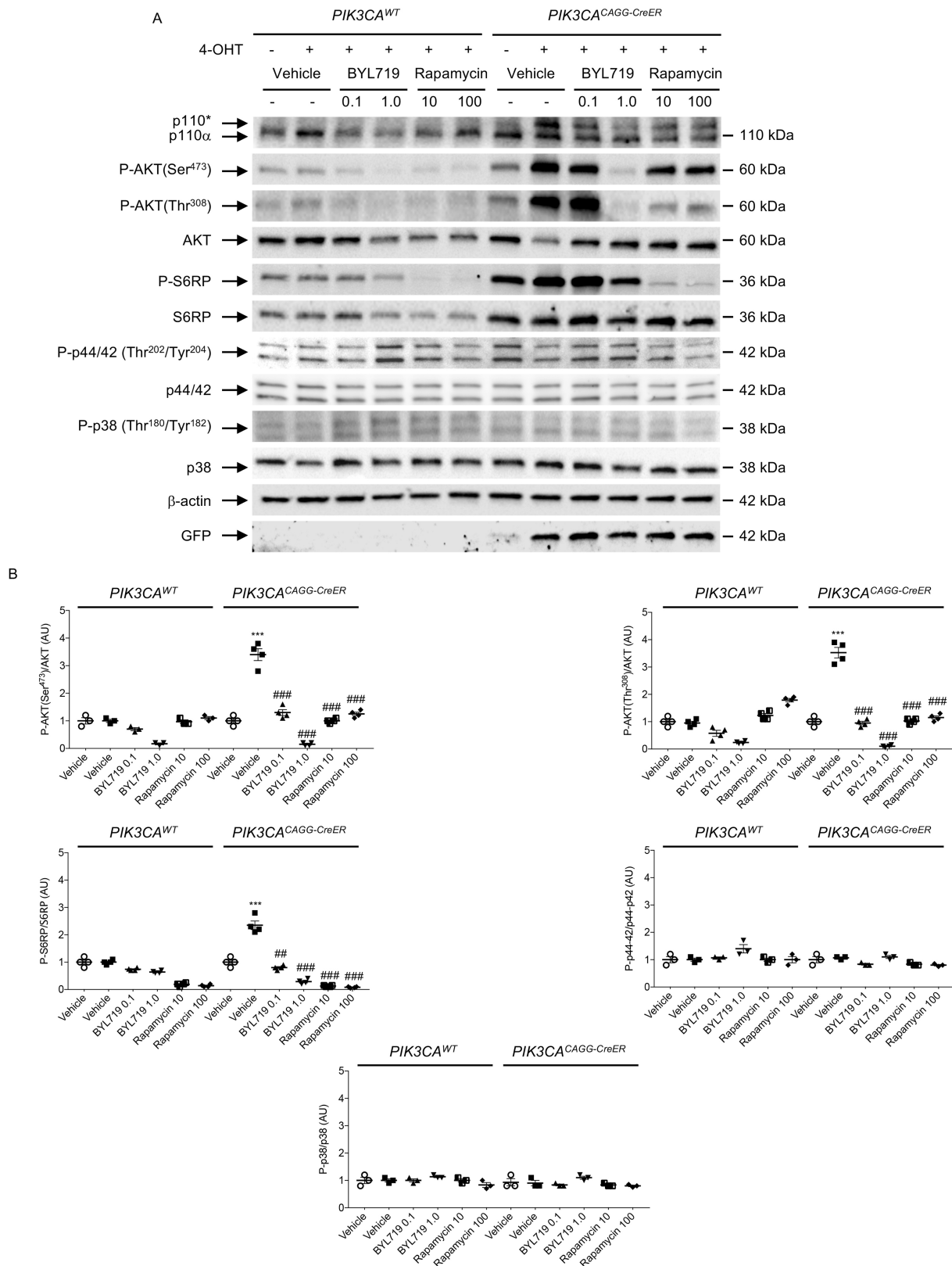
p110* versus wild-type p110, +++ $P < 0.001$. p110* versus p110* KD, \$\$\$ $P < 0.001$. Negative control is a vector that contains cDNA encoding GFP. **b**, Histological examination of different tissues from *PIK3CA*^{CAGG-CreER} mice. Left column, from top to bottom, liver, abdominal tumour, leg and ear abnormalities. Middle column, PAS or HE staining of the tissue. Right column, Ki67 staining of the same tissue ($n = 8$ mice). Scale bars, 20 μ m. **c**, Design of the experiment shown in Fig. 2h. *PIK3CA*^{CAGG-CreER} mice received a single dose of 4 mg kg⁻¹ tamoxifen and were followed for one month. Once the tumours became visible, BYL719 was started for two weeks and then withdrawn.





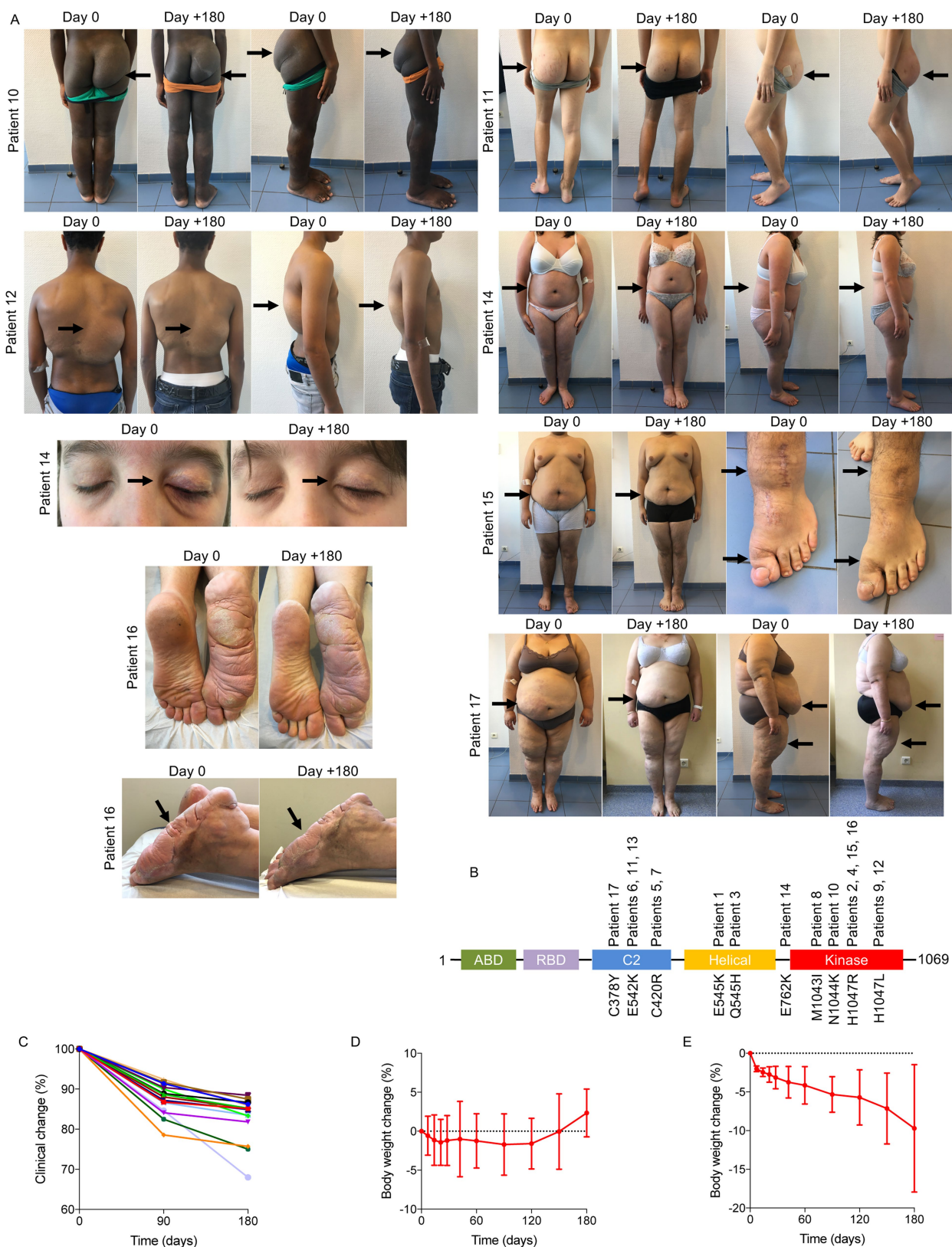
Extended Data Fig. 9 | Effect of rapamycin treatment on the different *PIK3CA*^{CAGG-CreER} mouse models. a, Kaplan–Meier survival curves of *PIK3CA*^{CAGG-CreER} mice that received a single dose of 40 mg kg^{−1} tamoxifen and were treated with or without rapamycin after tamoxifen administration. **b**, Representative pictures of the liver of *PIK3CA*^{CAGG-CreER} mice treated with rapamycin 40 days after *Cre* induction. **c**, Morphology of livers and spleens from *PIK3CA*^{WT} and *PIK3CA*^{CAGG-CreER} mice that were treated with or without rapamycin after *Cre* induction. Scale bars, 10 μm. **d**, Western blot and quantification of P-AKT (Ser⁴⁷³) and P-S6RP in the

liver, heart and muscle, respectively, of *PIK3CA*^{WT} and *PIK3CA*^{CAGG-CreER} mice treated with vehicle or rapamycin directly after *Cre* induction. **e**, *PIK3CA*^{CAGG-CreER} mice were treated with rapamycin one month after *Cre* induction with a single dose of 4 mg kg^{−1} tamoxifen and followed for one month. All data are shown as mean ± s.e.m. ANOVA followed by Tukey–Kramer test (two-tailed). *PIK3CA*^{CAGG-CreER} versus *PIK3CA*^{WT} mice, ****P* < 0.001. *PIK3CA*^{CAGG-CreER} mice treated with rapamycin compared with *PIK3CA*^{CAGG-CreER} mice treated with vehicle, ###*P* < 0.001.



Extended Data Fig. 10 | In vitro effect of BYL719 and rapamycin on fibroblasts from *PIK3CA*^{CAGG-CreER} mice. a, Skin fibroblasts from *PIK3CA*^{WT} and *PIK3CA*^{CAGG-CreER} mice were isolated and exposed to vehicle or increasing concentrations of BYL719 or rapamycin for 24 h. **b,** Quantification. White column, without 4-OHT; black column, with

4-OHT. All data are shown as mean ± s.e.m. ANOVA followed by Tukey-Kramer test (two-tailed). Before versus after *Cre* induction with 4-OHT, ****P* < 0.001. BYL719 or rapamycin exposure compared with cells treated with vehicle, ***P* < 0.01 and ###*P* < 0.001.

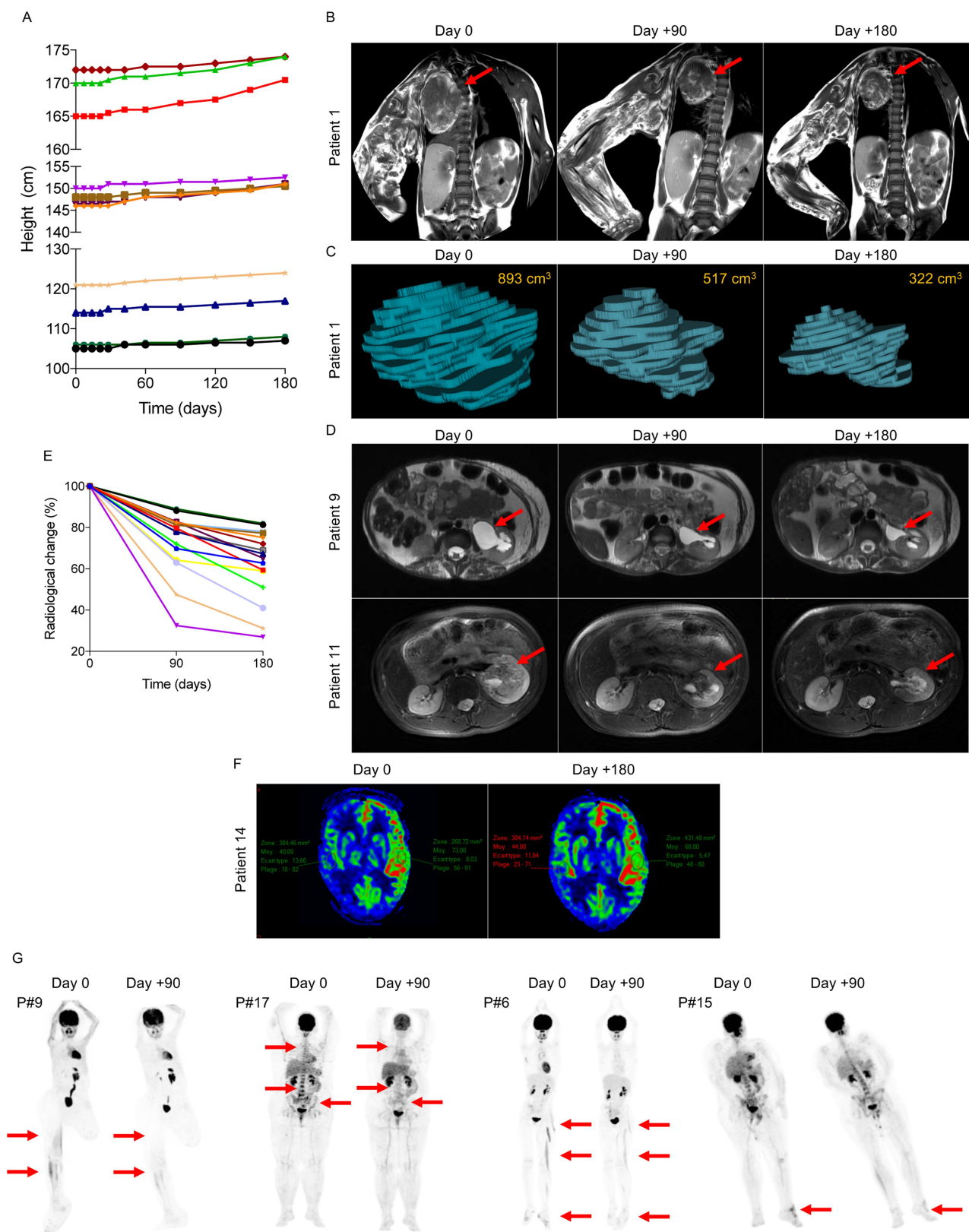


Extended Data Fig. 11 | See next page for caption.

Extended Data Fig. 11 | Effect of BYL719 in patients with PROS.

a, Patients 10–17 before and after 180 days of BYL719 treatment. Patient 10 was a 14-year-old boy with severe asthenia, dyspnea and bilateral overgrowth of lower limbs. After 180 days of treatment asthenia resolved and we observed a marked reduction in hypertrophy of the limbs. Patient 11 was a 14-year-old boy with overgrowth of the right buttock and an intra-abdominal vascular tumour infiltrating the left kidney and spinal nerve. He had chronic haematuria and was permanently confined to bed owing to pain. After 180 days, haematuria resolved and the volume of the intraabdominal vascular malformation was reduced by up to 68%. He had no more pain and became capable of walking. Patient 12 was a 15-year-old boy with multiple large tumours of the trunk and the back. After 180 days of treatment the tumours had reduced in size. Patient 13 was a 16-year-old boy with megalencephaly-capillary malformation (MCAP) and left hemifacial hyperplasia. Treatment led to a reduction in hemifacial hypertrophy and cognitive improvement. Owing to the deformation, this patient was not able to open the left eye. After 180 days of BYL719 treatment, he was able to open the eye (not shown for confidentiality reasons). Patient 14 was a 16-year-old girl with MCAP and a chronic noninfectious palpebral cellulitis who was steroid-dependent. BYL719 treatment led to the healing of the cellulitis and steroids were

stopped without a flare. We also observed enhancement of cognitive function and behaviour and improvement of scoliosis. Patient 15 was a 19-year-old man with overgrowth of the left foot and unstable and painful walking. Treatment led to an improvement in the overgrowth as well as an improvement in walking distance. Patient 16 was a 32-year-old man with overgrowth of the right foot and unstable and painful walking. Treatment led to an improvement in the overgrowth as well as an improvement in walking distance. Patient 17 was 50-year-old woman with generalized hypertrophy, and severe and diffuse pain with opioid dependency. She was permanently confined to bed. After six months of treatment we observed an improvement in tiredness, and resolution of pain, and we were able to stop opioids within two weeks. The patient became able to walk again. **b**, *PIK3CA* mutations identified in the 17 patients. **c**, For each patient we determined a target lesion (see Supplementary Table 2) that was clinically measured at each time point. The graph represents the changes (per cent) during the 180 days of treatment with BYL719. Each line is a single patient. **d**, Mean body weight changes (per cent) during the 180 days of treatment with BYL719 ($n = 13$ patients, patients 1–13), excluding the four obese patients (patients 14, 15, 16 and 17). **e**, Mean body weight loss in the four obese patients during the 180 days of treatment with BYL719. All data are shown as mean \pm s.e.m.



Extended Data Fig. 12 | Height changes in children during treatment period and radiological changes with BYL719 treatment. **a**, Height changes in children during the 180 days of treatment with BYL719. **b**, MRI scans of patient 1 before and after 180 days of BYL719 treatment. Arrows show the target lesion. **c**, Three-dimensional MRI-based reconstruction of the chest tumour in patient 1 before and after 180 days of BYL719 treatment. **d**, Examples of MRI showing the evolution of the target lesions

in patients 9 and 11. **e**, Volume evolution of the radiological target lesion after 180 days of BYL719 treatment. **f**, Diffusion MRI demonstrating the enhancement of brain perfusion in patient 14 after 180 days of BYL719. **g**, PET scan images of patients 6, 9, 15 and 17, before and after 90 days of BYL719 treatment. The arrows delineate hypermetabolic activity before and after 90 days of treatment.

Reporting Summary

Nature Research wishes to improve the reproducibility of the work that we publish. This form provides structure for consistency and transparency in reporting. For further information on Nature Research policies, see [Authors & Referees](#) and the [Editorial Policy Checklist](#).

Statistical parameters

When statistical analyses are reported, confirm that the following items are present in the relevant location (e.g. figure legend, table legend, main text, or Methods section).

n/a Confirmed

- ☐ ☒ The exact sample size (n) for each experimental group/condition, given as a discrete number and unit of measurement
- ☐ ☒ An indication of whether measurements were taken from distinct samples or whether the same sample was measured repeatedly
- ☐ ☒ The statistical test(s) used AND whether they are one- or two-sided
Only common tests should be described solely by name; describe more complex techniques in the Methods section.
- ☒ ☐ A description of all covariates tested
- ☐ ☒ A description of any assumptions or corrections, such as tests of normality and adjustment for multiple comparisons
- ☐ ☒ A full description of the statistics including central tendency (e.g. means) or other basic estimates (e.g. regression coefficient) AND variation (e.g. standard deviation) or associated estimates of uncertainty (e.g. confidence intervals)
- ☐ ☒ For null hypothesis testing, the test statistic (e.g. F , t , r) with confidence intervals, effect sizes, degrees of freedom and P value noted
Give P values as exact values whenever suitable.
- ☒ ☐ For Bayesian analysis, information on the choice of priors and Markov chain Monte Carlo settings
- ☒ ☐ For hierarchical and complex designs, identification of the appropriate level for tests and full reporting of outcomes
- ☐ ☒ Estimates of effect sizes (e.g. Cohen's d , Pearson's r), indicating how they were calculated
- ☐ ☒ Clearly defined error bars
State explicitly what error bars represent (e.g. SD, SE, CI)

Our web collection on [statistics for biologists](#) may be useful.

Software and code

Policy information about [availability of computer code](#)

Data collection

Provide a description of all commercial and custom code used to collect the data in this study, specifying the version used OR state that no software was used.

Data analysis

Graph Prism software

For manuscripts utilizing custom algorithms or software that are central to the research but not yet described in published literature, software must be made available to editors/reviewers upon request. We strongly encourage code deposition in a community repository (e.g. GitHub). See the Nature Research [guidelines for submitting code & software](#) for further information.

Data

Policy information about [availability of data](#)

All manuscripts must include a [data availability statement](#). This statement should provide the following information, where applicable:

- Accession codes, unique identifiers, or web links for publicly available datasets
- A list of figures that have associated raw data
- A description of any restrictions on data availability

Provide your data availability statement here.

Field-specific reporting

Please select the best fit for your research. If you are not sure, read the appropriate sections before making your selection.

☒ Life sciences

☐ Behavioural & social sciences

For a reference copy of the document with all sections, see [nature.com/authors/policies/ReportingSummary-flat.pdf](https://www.nature.com/authors/policies/ReportingSummary-flat.pdf)

Life sciences

Study design

All studies must disclose on these points even when the disclosure is negative.

Sample size

Data exclusions

Replication

Randomization

Blinding

Materials & experimental systems

Policy information about [availability of materials](#)

n/a ☐ Involved in the study

☐ Unique materials

☐ Antibodies

☒ Eukaryotic cell lines

☐ Research animals

☐ Human research participants

Unique materials

Obtaining unique materials

Describe any restrictions on the availability of unique materials OR confirm that all unique materials used are readily available from the authors or from standard commercial sources (and specify these sources).

Antibodies

Antibodies used

Paraffin-embedded kidney sections (4- m) were incubated with anti-P-AKT (Ser473) antibody (Cell Signaling Technology, ref# 4060, dilution 1:100), anti-P-S6RP antibody (Cell Signaling Technology, ref# 5364, dilution 1:100), anti- -smooth muscle cell antibody (Sigma Aldrich, ref# A5228, dilution 1:100), anti-CD34 antibody (eBioscience, ref# 14-0341, dilution 1:100), anti-CD31 antibody (Dianova, ref# Dia-310, dilution 1:30) and anti-podoplanin antibody (Agilent, ref#M3619, dilution 1:50). Western blots were performed as previously described³⁰. Briefly, protein extracts from the liver, muscles, heart, kidneys and fibroblasts were resolved by SDS-PAGE before being transferred onto the appropriate membrane and incubated with anti-P-AKT (Ser473) antibody (Cell Signaling Technology, ref# 4060, dilution 1:1000), anti-P-AKT (Thr308) antibody (Cell Signaling Technology, ref# 13038, dilution 1:1000), anti- AKT antibody (Cell Signaling Technology, ref# 9272, dilution 1:1000), anti-P-S6RP antibody (Cell Signaling Technology, ref# 5364, dilution 1:1000), anti-p110 (Cell Signaling Technology, ref# 4249, dilution 1:1000), anti-LYVE-1 (R&D Systems, ref# AF2125, dilution 1:1000), anti-P-p44/42 antibody (Cell Signaling Technology, ref# 4370, dilution 1:1000), anti-p44/42 (Thr202/Tyr204) antibody (Cell Signaling Technology, ref# 9102, dilution 1:1000), anti-P-p38 (Thr180/Tyr182) antibody (Cell Signaling Technology, ref# 9216, dilution 1:1000), anti-p38 antibody (Cell Signaling Technology, ref# 8690, dilution 1:1000), anti-GFP antibody (Abcam, ref# ab13970, dilution 1:1000), anti-GAPDH (Merck Millipore, ref#374, dilution 1:1000) or anti- actin antibody (Sigma-Aldrich, ref#A2228, dilution 1:1000), followed by the appropriate peroxidase-conjugated secondary antibody (dilution 1:10000).

Validation

Describe the validation of each primary antibody for the species and application, noting any validation statements on the manufacturer's website, relevant citations, antibody profiles in online databases, or data provided in the manuscript.

Research animals

Policy information about [studies involving animals](#); [ARRIVE guidelines](#) recommended for reporting animal research

Animals/animal-derived materials

For this study, we interbred homozygous R26StopFLP110* (Stock# 012343) and heterozygous CAGGCre-ERTM (Stock# 004682) mice on the C57BL/6 background obtained from Jackson Laboratories. We obtained R26StopFLP110*^{+/+} x CAGGCre-ERTM⁺ mice (referred here as PIK3CACAGG-CreER mice) and R26StopFLP110*^{+/+} x CAGGCre-ERTM⁻ mice (referred here as PIK3CAWT mice). We used the p110* construction published by Klippel A. et al¹⁷ (Supplementary Fig.1). The p110* protein is a constitutively active chimera that contains the iSH2 domain of p85 fused to the NH2-terminus of p110 via a flexible glycine-linker. To generate tissue-specific p110*-transgenic mice, a cloned loxP-flanked neoR-stop cassette was inserted into a modified version of pROSA26-1 followed by the cDNA encoding p110* and then a frt-flanked IRES-EGFP cassette and a bovine polyadenylation sequence (R26StopFLP110*)¹⁶.

Animals were fed ad libitum and housed at a constant ambient temperature in a 12-hour light cycle. Animal procedures were approved by the "Services Vétérinaires de la Préfecture de Police de Paris" Departmental Director and by the ethical committee of the Paris Descartes University. In the first study, a single dose of tamoxifen (40 mg.kg⁻¹) was administered through oral gavage when the mice were at 21 days of age. For the survival studies, the mice were followed daily after tamoxifen gavage (PIK3CAWT n=16 and PIK3CACAGG-CreER n=16). For the preventive studies, the mice were treated with the PI3KCA inhibitor, BYL719 (MedChem Express; 50 mg.kg⁻¹ in 0.5% carboxymethylcellulose (Sigma Aldrich), daily p.o.) (n=16) or vehicle (0.5% carboxymethylcellulose (Sigma Aldrich), daily p.o.) (n=16). For the therapeutic studies, the mice were treated with the PI3KCA inhibitor, BYL719 (MedChem Express; 50 mg.kg⁻¹ in 0.5% carboxymethylcellulose (Sigma Aldrich), daily p.o.) (n=12) or vehicle (0.5% carboxymethylcellulose (Sigma Aldrich), daily p.o.) (n=12). Treatment was started at the same time of tamoxifen gavage, for the preventive study, or seven days after, for the therapeutic study.

In the second study, a single dose of tamoxifen (4 mg.kg⁻¹) was administered through oral gavage when the mice were at 21 days of age (PIK3CACAGG-CreER n=28). Ten mice were sacrificed at approximately 1 month post tamoxifen gavage when tumors reached a certain volume for tissues examination. Once gross morphological abnormalities were visible, eighteen mice were treated with BYL719 during 15 days and treatment was stopped once macroscopic lesions disappeared to follow their phenotype.

In the third study, a single dose of tamoxifen (40 mg.kg⁻¹) was administered through oral gavage when the mice were at 21 days of age and then were treated with daily intraperitoneal injection of rapamycin (MedChem Express, ref#HY-10219) (PIK3CACAGG-CreER n=7) or vehicle (PIK3CACAGG-CreER n=7) during 30 days. Rapamycin was dissolved to a final concentration of 0.5 mg.ml⁻¹ in absolute ethanol dissolved further in 5% polyethylene glycol (PEG-400) and 5% Tween 80 in PBS and used for intraperitoneal injection at 4 mg.kg⁻¹. All mice treated with rapamycin or vehicle were then sacrificed for tissues examination.

In the fourth study, a single dose of tamoxifen (4 mg.kg⁻¹) was administered through oral gavage when the mice were at 21 days of age (PIK3CACAGG-CreER n=6). Once gross morphological abnormalities were visible (approximately 30 days later), all the mice were treated with daily intraperitoneal injection of rapamycin (MedChem Express, ref#HY-10219) during 30 days. Rapamycin was dissolved to a final concentration of 0.5 mg/ml in absolute ethanol dissolved further in 5% polyethylene glycol (PEG-400) and 5% Tween 80 in PBS and used for intraperitoneal injection at 4 mg.kg⁻¹.

Human research participants

Policy information about [studies involving human research participants](#)

Population characteristics

The study was conducted on 19 patients, 4 adults and 15 children, followed at Necker hospital. This protocol was approved by the "Agence Nationale de Sécurité du Médicament et des Produits de Santé" (ANSM, authorizations n°: 553984-986, 584018, 585881-586135, 585464, 585465, 585467, 585880, 586136, 585463, 596229, 588018, 587904, 587896-912, 587908, 587905, 587910, 585458, 595374, 587899) and informed written consent was obtained from the adult patient and the legal representatives of the child. BYL719 was compassionately offered by Novartis. Adult patients received 250 mg/day and child patients received 50 mg/day. BYL719 was orally delivered every morning before breakfast.

Patients were followed at regular intervals: weekly during 8 weeks, every two weeks during 1 month and then monthly. Glycaemia was evaluated daily the first month and then progressively sparse. At all time points, the patients had a physical examination and performance status measurement using the Karnofsky (on a scale from 0 to 100, with lower numbers indicating greater disability) and the ECOG indexes (a scale of 0 to 5, with 0 indicating no symptoms and higher scores indicating increasing symptoms)^{25,26}. Growth of the children was monitored at all clinical appointments. Blood sampling (complete blood count, kidney and liver functions, glycated hemoglobin measurement) were performed at each time points. Glycaemia was monitored after all meals over two months and then the monitoring became progressively sparse. Adverse events were graded according to National Cancer Institute Common Terminology Criteria for Adverse Events, version 4.0. All patients had heart ultrasound before BYL719 and then every 3 months. Magnetic resonance imaging studies were performed before BYL719 introduction and then at 3 and 6 months of treatment. PET-scan were performed before and at 3 months of treatment.

Method-specific reporting

n/a	Involved in the study
<input checked="" type="checkbox"/>	<input type="checkbox"/> ChIP-seq
<input type="checkbox"/>	<input checked="" type="checkbox"/> Flow cytometry
<input type="checkbox"/>	<input checked="" type="checkbox"/> Magnetic resonance imaging

Flow Cytometry

Plots

Confirm that:

- ☒ The axis labels state the marker and fluorochrome used (e.g. CD4-FITC).
- ☒ The axis scales are clearly visible. Include numbers along axes only for bottom left plot of group (a 'group' is an analysis of identical markers).
- ☒ All plots are contour plots with outliers or pseudocolor plots.
- ☒ A numerical value for number of cells or percentage (with statistics) is provided.

Methodology

Sample preparation

Spleens of PIK3CAWT (n=12), PIK3CACAGG-CreER induced with tamoxifen 40 mg.kg⁻¹ (n=6) and PIK3CACAGG-CreER induced with tamoxifen 4 mg.kg⁻¹ (n=6) mice were mechanically disrupted in PBS/SVF 2%. Following dissociation, spleens were filtered, centrifuged and resuspended. Cells were then treated with a FC blocker for 10 min at 4°C (Biolegend, ref# 101302) and fixed/permeabilized (BD Bioscience, ref# 554714). Cells were labeled with chicken polyclonal anti-GFP antibody (Abcam, ref# ab13970) for 30 min at 4°C. Subsequently, cells were incubated with Alexa Fluor 647-labeled goat anti-chicken IgY antibody (Abcam, ref# ab150171) for 30 min at 4°C. A background control incubated only with secondary antibody was also included.

Instrument

Samples were analyzed using Gallios™ Flow Cytometer (Beckman Coulter)

Software

FlowJo software (TreeStar)

Cell population abundance

Describe the abundance of the relevant cell populations within post-sort fractions, providing details on the purity of the samples and how it was determined.

Gating strategy

Describe the gating strategy used for all relevant experiments, specifying the preliminary FSC/SSC gates of the starting cell population, indicating where boundaries between "positive" and "negative" staining cell populations are defined.

- ☒ Tick this box to confirm that a figure exemplifying the gating strategy is provided in the Supplementary Information.

Magnetic resonance imaging

Experimental design

Design type

MRI were performed at the Plateforme IRM, INSERM U970, Centre de recherche cardiovasculaire de Paris. Briefly, MRI were performed under general anesthesia in 4 weeks old female PIK3CAWT (n=6) and PIK3CACAGG-CreER (n=6) mice that received 7 days before a single dose of 40 mg.kg⁻¹ tamoxifen to induce Cre recombination. MRI were then repeated weekly in all mice during 1 month.

Design specifications

Specify the number of blocks, trials or experimental units per session and/or subject, and specify the length of each trial or block (if trials are blocked) and interval between trials.

Behavioral performance measures

State number and/or type of variables recorded (e.g. correct button press, response time) and what statistics were used to establish that the subjects were performing the task as expected (e.g. mean, range, and/or standard deviation across subjects).

Acquisition

Imaging type(s)

Whole body MRI

Field strength

Specify in Tesla

Sequence & imaging parameters

T1, T2

Area of acquisition

Whole body MRI

Diffusion MRI

☐ Used

☒ Not used

Preprocessing

Preprocessing software

Provide detail on software version and revision number and on specific parameters (model/functions, brain extraction, segmentation, smoothing kernel size, etc.).

Normalization

If data were normalized/standardized, describe the approach(es): specify linear or non-linear and define image types used for transformation OR indicate that data were not normalized and explain rationale for lack of normalization.

Normalization template

Describe the template used for normalization/transformation, specifying subject space or group standardized space (e.g. original Talairach, MNI305, ICBM152) OR indicate that the data were not normalized.

Noise and artifact removal

Describe your procedure(s) for artifact and structured noise removal, specifying motion parameters, tissue signals and physiological signals (heart rate, respiration).

Volume censoring

Define your software and/or method and criteria for volume censoring, and state the extent of such censoring.

Statistical modeling & inference

Model type and settings

Specify type (mass univariate, multivariate, RSA, predictive, etc.) and describe essential details of the model at the first and second levels (e.g. fixed, random or mixed effects; drift or auto-correlation).

Effect(s) tested

Define precise effect in terms of the task or stimulus conditions instead of psychological concepts and indicate whether ANOVA or factorial designs were used.

Specify type of analysis: ☐ Whole brain ☒ ROI-based ☐ Both

Anatomical location(s)

Statistic type for inference
(See [Eklund et al. 2016](#))

Specify voxel-wise or cluster-wise and report all relevant parameters for cluster-wise methods.

Correction

Describe the type of correction and how it is obtained for multiple comparisons (e.g. FWE, FDR, permutation or Monte Carlo).

Models & analysis

n/a	Involvement in the study
<input type="checkbox"/>	<input type="checkbox"/> Functional and/or effective connectivity
<input checked="" type="checkbox"/>	<input type="checkbox"/> Graph analysis
<input checked="" type="checkbox"/>	<input type="checkbox"/> Multivariate modeling or predictive analysis

Functional and/or effective connectivity

Report the measures of dependence used and the model details (e.g. Pearson correlation, partial correlation, mutual information).